Thermal decomposition of the reduced porphyrin species in the gas phase (Bn in Scheme II), but most importantly on the source surfaces (An in Scheme II), is proposed as the mechanism of formation for the major pyrrolic ions (as well as the majority of other fragments) observed in the CI mass spectra. Since, at high source temperatures (>673 K), the porphyrin macrocycle will decompose,[9] is it probable that the reduced porphyrin species, which have a less stable macrocycle than the porphyrin, are very susceptible to thermal decomposition at the temperatures employed in the present studies.

Production of the major pyrrolic fragment ions through a thermal decomposition mechanism is strongly supported by the desorption profiles shown in Figure 3. These profiles demonstrate that the majority of the reduced species and pyrrolic fragments observed in the CI mass spectra are formed from porphyrin species that condense on the source walls. These products formed from surface-bound porphyrin are observed to increase in relative abundance with time in the ion source and reach their maximum intensity after the DCI current (temperature) has reached its maximum level and continues to radiatively heat the source surfaces. As the DCI probe heats the surfaces, the less stable reduced species on the surfaces are thermally decomposed and the resulting neutral pyrrolic species can vaporize, possibly undergoing additional reactions in the CI plasma, before being ionized. (Thermal decomposition of material introduced using a DCI probe and the "double maxima" phenomena in DCI desorption profiles have been noted for other compound classes.[26]) Similar arguments can be made for the case in which the porphyrin is placed on the ion source repeller plate prior to the analysis (Figure 1a-c). The percentage of the reduced species formed on the source surfaces that decomposes, rather than vaporizing intact, increases as the ion source temperature increases. (This is also true when the direct insertion probe or DCI probe is used to introduce the sample.) Fragment ion abundance increases in these spectra as the ion source temperature increases, and pyrrolic fragment ions are observed in the spectra obtained at high source temperatures even though little or no reduced species are evident (i.e., there is total thermal decomposition of the (M + nH) species).

(26) Cotter, R. J. *Anal. Chem.* **1980**, *52*, 1589A-1606A.

Conclusions

Previously proposed reduction/decomposition mechanisms, invoking a gas-phase ion-molecule reduction scheme and unimolecular decomposition of the ionized reduction products, cannot fully account for the appearance of high-pressure CI mass spectra of porphyrins. The results from this study demonstrate that the phenomena responsible for the appearance of these high-pressure CI mass spectra are different than previously proposed.

The porphyrin reduction observed in a high-pressure CI plasma *does not* result from gas-phase ion-molecule chemistry. Radical hydrogen, rather than neutral or ionized reagent gas species, appears to be the most likely reducing agent, and the reduction is surface-assisted. Furthermore, the reduction process is largely independent of reagent gas, as long as a source of radical hydrogen is present.

Simple unimolecular decomposition of the reduced porphyrin species (e.g., $(M + 7H)^+$) *does not* produce the most abundant pyrrolic fragment ions observed in high-pressure CI mass spectra. This decomposition pathway can contribute, however, to the overall CI mass spectrum. The amount of this contribution is largely dependent on the energetics of the ionization process, and, therefore, the CI reagent gas. For example, less fragmentation is observed in ammonia CI mass spectra than hydrogen CI mass spectra, at the same ion source temperature, because of the lower exothermicity of ionization when using ammonia. The most abundant fragment ions, as well as the majority of the fragment ions, observed in the high-pressure CI mass spectra more likely originate via thermal decomposition of the reduced porphyrin species in the gas phase, but most importantly on the source surfaces, producing neutral pyrrolic units that possibly undergo additional reactions in the CI plasma prior to ionization. Therefore, the relative abundance of the different ions and the amount of fragmentation observed in the high-pressure CI mass spectra, when using a particular porphyrin and reagent gas, will correlate with the temperature of the ion source.

Acknowledgment. This work was supported by the U.S. Department of Energy, Office of Basic Energy Sciences, through Contract DE-AC05-840R21400 with Martin Marietta Energy Systems, Inc.

Multiphoton Ionization of Acetone Clusters: Metastable Unimolecular Decomposition of Acetone Cluster Ions and the Influence of Solvation on Intracluster Ion-Molecule Reactions

W. B. Tzeng, S. Wei, and A. W. Castleman, Jr.*

Contribution from the Department of Chemistry, The Pennsylvania State University, University Park, Pennsylvania 16802. *Received February 27, 1989*

Abstract: A comprehensive investigation of the reactions of acetone ions in clusters was made to investigate and compare the similarities and differences in the ion reactions due to solvation effects. Neutral acetone clusters, prepared in a pulsed nozzle supersonic expansion, are ionized using multiphoton ionization and investigated using a time-of-flight reflectron technique. The observed major cluster ions resulting from prompt fragmentation following ionization are $[(CH_3)_2CO]_m \cdot H^+$ (m = 1-15), $[(CH_3)_2CO]_m \cdot C_2H_3O^+$ (m = 1-17), and $[(CH_3)_2CO]_m \cdot CH_3^+$ (m = 1-10). In a time window of a few tens of microseconds, all three classes of cluster ions unimolecularly decompose, losing only one acetone monomer. Interestingly, a reaction corresponding to the dehydration of $[(CH_3)_2CO]_m \cdot H^+$ and leading to the production of $[(CH_3)_2CO]_{m-2} \cdot C_6H_{11}O^+$ is observed for m = 2-6. The most striking finding of the present study is that the presence of water molecules in a cluster suppresses the dehydration reaction. This finding clarifies the discrepancy between earlier studies reported in the literature and, most importantly, provides further evidence for the influence of a solvent on ion reactions in clusters, and ion-molecule reactions in general.

Unraveling the influence of solvation on chemical reactions is a topic of considerable current interest. It is recognized that insight into reasons for similarities and differences in reactivity between the gaseous state and the condensed state can be gained by studying reactivities of clusters as a function of the degree of aggregation. Acetone is a widely used solvent, and studies of acetone clusters serve as a good model for unraveling reactions of hydrogen-bonded organic systems with specific reference to

0002-7863/89/1511-6035$01.50/0

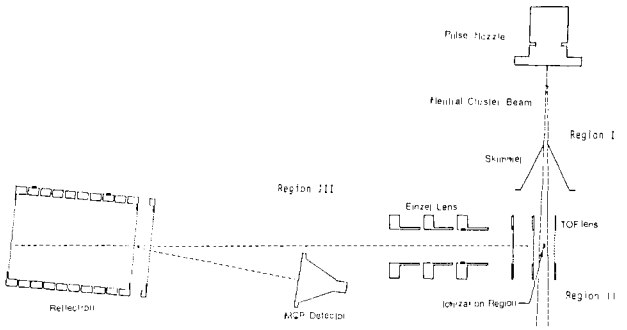

Figure 1. Schematic of the laser multiphoton ionization time-of-flight mass spectrometer with reflectron.

differences between the gas phase and the condensed state.[1-7] While the overall thrust of the work was to investigate the influence of solvation on reactions of the acetone ion, the principal objectives of the present study are 3-fold: (1) determine whether the same main ions dominate in acetone solvated clusters as in those formed in isolated binary reactions; (2) compare the inferred structures of cluster ions formed in association reactions with those produced upon cluster ionization; and (3) ascertain whether the presence of a water molecule could influence reported dehydration reactions in these systems.

Results from experiments of ion–molecule reactions[8-12] of gaseous acetone have shown that $[(CH_3)_2CO]_m{\cdot}H^+$, $[(CH_3)_2CO]_m{\cdot}C_2H_3O^+$, ($[(CH_3)_2CO]_m{\cdot}CH_3^+$ (m = 1–4) are the cluster ion products resulting from the reactions between the primary ions, $C_2H_3O^+$, $(CH_3)_2CO^+$, CH_3^+, and the neutral acetone molecule. In addition, ions at masses 99, 157, and 215, which correspond to loss of a water molecule from the protonated dimer, trimer, and tetramer ions, have also been observed. However, in studies in which the neutral clusters of acetone were ionized, Stace and Shukla[13] found no evidence for ions corresponding to $C_6H_{11}O^+$ (mass 99) or $[(CH_3)_2CO]_m{\cdot}C_6H_{11}O^+$, which would correspond to 157 (m = 1) and 215 (m = 2). They suggested that the difference in the results between the isolated gas-phase ion–molecule reaction studies and those involving cluster ionization is due to a different route to the formation of their precursor ions, $[(CH_3)_2CO]_m{\cdot}H^+$.

The present work involves the use of a multiphoton ionization time-of-flight mass spectrometer (TOFMS), equipped with a reflection, to investigate the dehydration mechanism of $[(CH_3)_2CO]_m{\cdot}H^+$ and also study the unimolecular decomposition processes of the cluster ions $[(CH_3)_2CO]_m{\cdot}H^+$, $[(CH_3)_2CO]_m{\cdot}C_2H_3O^+$, and $[(CH_3)_2CO]_m{\cdot}CH_3^+$. (Hereafter, T will be used to designate the acetone moiety.) The experimental results also provide information on branching ratios in prompt fragmentation processes, the size distributions of clusters, and relative stabilities of solvated acetone cluster ions.

Experimental Section

The apparatus used in these studies is a modified version of one described in detail in a previous publication.[14] The major modification is that a reflection has been added to the laser photoionization time-of-flight mass spectrometer. Equipped with the reflectron, the present apparatus can be used to investigate metastable decomposition processes of cluster ions. Therefore, information on the dissociation dynamics of cluster ions can be extracted.

The major components of the apparatus are shown in Figure 1. Neutral acetone clusters are formed by an argon seeded supersonic expansion of acetone vapor from a pulsed nozzle source. Base pressure in the ionization chamber (Region II) is normally around 2×10^{-7} Torr. With a 150-μm diameter nozzle and a stagnation pressure of 5 atm, the chamber pressure is raised to no more than 4×10^{-6} Torr under normal experimental conditions. The neutral clusters are ionized by 355-nm light from a frequency-tripled Nd:YAG laser. Cluster ions formed by the multiphoton ionization process are accelerated in a double electrostatic field[15] to about 2 keV and directed through a 130-cm long field-free region toward the reflectron. Ions are then reflected at an overall angle of 3° and thereafter travel 85 cm through another field-free region toward a chevron microchannel plate detector.

The reflectron, based on the design by Mamyrin et al.,[16] consists of 10 stainless steel rings (7.50 cm o.d. × 6.25 cm i.d.) which are positioned with alumina spacers (Kimball Physics, Inc.). In order to maintain field uniformity, the central portions of the first two and the last ring are affixed with screens comprised of 90% transmission nickel meshes. The first two pieces making up the ion deceleration, and daugther ion reflection field are spaced 1.50 cm apart; the length from the second to the last cylinder is 11.5 cm. The whole reflectron assembly is mounted on a two-dimensional rotatable block (Newport Research Corp., Model 481) which provides fine adjustment for the reflection angle. Each of the two angle adjustment knobs is coupled to a driving shaft through a vacuum chamber flange. Thus, the angular tuning of the reflectron unit can be done outside the vacuum chamber. Since once reflected the daughter and parent ions penetrate into different regions of the reflectron, they have different trajectories to the detector. Hence, the initial alignment and the availability of the two-dimensional angle adjustment of the reflectron are very critical in deducing cluster ion distribution and daughter–parent ion intensity ratio measurements.

Two experiments have been performed to verify that collision-induced dissociation of cluster ions is negligible under the normal operation conditions. An experiment was conducted to investigate if there are any cluster ions formed due to the collision between the photoionized species and the scattered acetone gas in the ionization and ion acceleration regions. The time-of-flight spectra have been taken for very low concentrations (less than 1 ppm) of acetone in helium. Since the $(T)_m{\cdot}H^+$, m = 1–4, species are observed under this condition, one can be confident that these species are not product ions resulting from collisional processes. Secondly, we observed the change in the daughter and parent ion intensity ratios while varying the chamber pressure of field-free region in the range of 7×10^{-7} to 7×10^{-6} Torr. This is a standard procedure for examining the contributions of collision-induced dissociation to the metastable decomposition processes.[17] The result shows that the daughter to parent ion intensity ratio remains invariant as long as the chamber pressure is below 1×10^{-6} Torr. The chamber pressure in the field-free and detector regions (Region III) has been maintained to be 2×10^{-7} Torr during normal experimental conditions, and collisional processes are negligible in the field-free region.

In studies made to investigate the metastability of cluster ions, the reflectron was used as an energy analyzer.[18] The initial ion energy (U_0), which is established by the potentials applied to the time-of-flight lens elements, can be measured by observing the change in the parent ion signal while varying the voltage (U_t) on the middle plate of reflectron unit. In the present experiments, the birth potential U_0 has been determined to be 1825 ± 10 V. A similar method is used for the investigation of the metastability of cluster ions. In this case, if a metastable decomposition process occurs in the field-free region, the reflected daughter ions with mass M_d are collected by the detector while the parent ions of mass

(1) Gaines, G. A.; Donaldson, D. J.; Strickler, S. J.; Vaida, V. *J. Phys. Chem.* **1988**, *92*, 2762.
(2) Donaldson, D. J.; Gaines, G. A.; Vaida, V. *J. Phys. Chem.* **1988**, *92*, 2766.
(3) Costela, A.; Crespo, M. T.; Figuera, J. M. *J. Photochem.* **1986**, *34*, 165.
(4) Trott, W. M.; Blais, N. C.; Walters, E. A. *J. Chem. Phys.* **1978**, *69*, 3150.
(5) Stace, A. J. *J. Am. Chem. Soc.* **1985**, *107*, 755.
(6) Castleman, A. W.; Jr. In *Kinetics of Ion Molecule Reactions*; Ausloos, P., Ed.; Plenum Press: New York, 1979; p 295.
(7) Kebarle, P. In *Ion Molecule Reactions*; Franklin, J. L., Ed.; Plenum Press: New York, 1972, Vol. 1, p 315.
(8) Munson, M. S. B. *J. Am. Chem. Soc.* **1965**, *87*, 5313.
(9) Blair, A. S.; Harrison, A. G. *Can. J. Chem.* **1973**, *15*, 703.
(10) Luczynski, Z.; Wincel, H. *Int. J. Mass Spectrom. Ion Phys.* **1977**, *23*, 37.
(11) Sieck, L. W.; Ausloos, P. *Radiat. Res.* **1972**, *52*, 47–58.
(12) MacNeil, K. A. G.; Futrell, J. H. *J. Phys. Chem.* **1972**, *76*, 409.
(13) Stace, A. J.; Shukla, A. K. *J. Phys. Chem.* **1982**, *86*, 865.
(14) Breen, J. J.; Kilgore, K.; Tzeng, W. B.; Wei, S.; Keesee, R. G.; Castleman, A. W. *Jr. J. Chem. Phys.* **1989**, *90*, 11.
(15) Wiley, W. C.; McLaren, I. H. *Rev. Sci. Instrum.* **1955**, *26*, 1150.
(16) Mamyrin, B. A.; Karataev, V. I.; Shmikk, D. V.; Zagulin, V. A. *Sov. Phys. JETP* **1973**, *37*, 45.
(17) Kilgore, K.; Morgan, S.; Tzeng, W. B.; Castleman, A. W. Jr. Dissociation of Ammonia Cluster Ions Following Their Formation Via Multiphoton Ionization. *J. Chem. Phys.*, submitted.
(18) Echt, O.; Dao, P. D.; Morgan, S.; Castelman, A. W., Jr. *J. Chem. Phys.* **1985**, *82*, 4076.

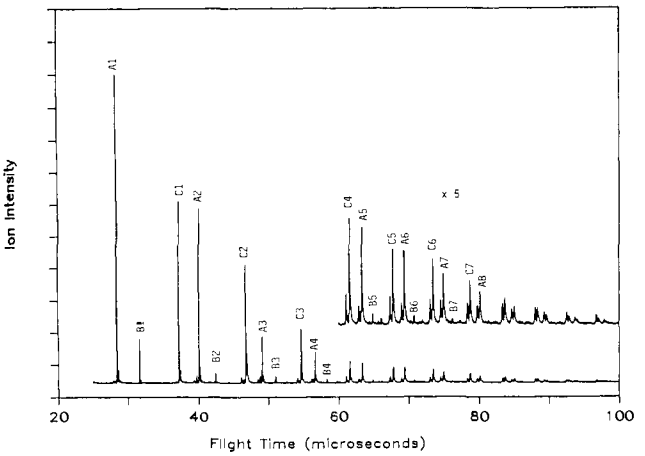

Figure 2. A typical time-of-flight mass spectrum of acetone cluster ions: nozzle diameter = 150 μm; stagnation pressure = 3600 Torr; 6% acetone in argon carrier gas. Am ≡ $(T)_m{\cdot}H^+$, Bm = $(T)_m{\cdot}CH_3^+$, and Cm ≡ $(T)_m{\cdot}C_2H_3O^+$.

M_p penetrate through the reflectron when $U_t < (M_d/M_p)U_0$.

The acetone used in these experiments is a certified ACS Spectranalyzed grade obtained from Fisher Scientific.

Results and Discussion

(A) Conventional (Time-of-Flight) Mass Spectra. When neutral acetone clusters are ionized through a multiphoton process, the following step will take place first:

$$(T)_m + nh\nu \rightarrow (T)_m^{+*} + e^- \qquad (1)$$

The excess energy upon ionization is partitioned into kinetic energy of the ejected electron and the internal energy of the ionic species $(T)_m^{+*}$. The internally excited $(T)_m^{+*}$ can then rearrange to form $(T)_m^+$ with a more stable structure, or alternatively fragment into $(T)_{m-1-x}{\cdot}H^+$, $(T)_{m-1-x}{\cdot}C_2H_3O^+$, and $(T)_{m-1-x}{\cdot}CH_3^+$ and other cluster ions. The inclusion of x designates the loss of intact acetone molecules from the cluster ion in addition to neutral fragments of the original acetone ion moiety undergoing intracluster ion–molecule reactions.

A conventional TOF spectrum records the final product ions which result after laser photoionization and ion fragmentation. Figure 2 is a time-of-flight spectrum of acetone clusters taken at a laser wavelength of 355 nm. For the results reported here, neutral acetone clusters were prepared by expanding the acetone–argon gas mixture through a pulsed nozzle at a stagnation pressure of 3600 Torr. It was found that relative cluster ion distributions are invariant with the laser power for values of 15–65 mJ/pulse; all experiments reported herein were made in that power regime.

(1) Major Cluster Ions. The observed major cluster ions are $(T)_m{\cdot}H^+$ (m = 1–15), $(T)_m{\cdot}C_2H_3O^+$, (m = 1–17), and $(T)_m{\cdot}CH_3^+$ (m = 1–10), whereas other cluster ions such as $(T)_m^+$ (m = 1–3), $(T)_m{\cdot}C_3H_5O^+$ (m = 1–12), and $(T)_m{\cdot}C_3H_3O^+$ (m = 1–5) are also present but only in small amounts.

Trott et al.[4] found that the ionization potentials of acetone clusters are a linear function in $1/m$, where m is number of acetone molecules. Based on the experimental measurements, they predicted a bulk ionization potential of about 8.8 eV; the ionization potentials of acetone monomer, dimer, trimer, and tetramer, are 9.694, 9.26, 9.10, and 9.02 eV, respectively.[4] The ionization is expected to be at least a three-photon process at the photon wavelength of 355 nm used in the present study. Under this condition, depending on the energy carried by the electron, excess energies of 0.78, 1.21, 1.37, and 1.46 eV respectively, for the four acetone clusters mentioned above are possible with an even greater value than 1.46 eV for the larger clusters. Even higher excess energies can be obtained if additional photons are absorbed.

The results of the present study show that most of the internally excited $(T)_m^{+*}$ ions fragment to form $(T)_{m-1-x}{\cdot}H^+$, $(T)_{m-1-x}{\cdot}C_2H_3O^+$, and $(T)_{m-1-x}{\cdot}CH_3^+$. The three major prompt fragmentation processes are expressed as follows:

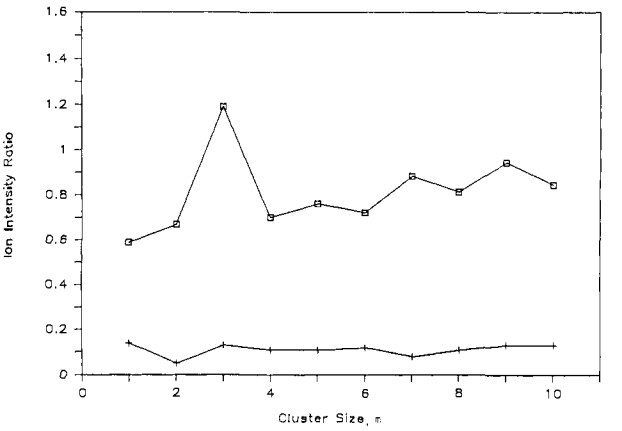

Figure 3. Cluster ion stability study as a function of cluster size. A plot of the relative ion intensities of $(T)_m{\cdot}CH_3^+$, $(T)_m{\cdot}C_2H_3O^+$, m = 1–10 as a function of number of solvent molecule, m: (□) $[(T)_m{\cdot}C_2H_3O^+]/[(T)_m{\cdot}H^+]$; (+) $[(T)_m{\cdot}CH_3^+]/[(T)_m{\cdot}H^+]$.

$$(T)_m^{+*} \rightarrow (T)_{m-1-x}{\cdot}H^+ + C_3H_5O + x(T) \qquad (2)$$

$$(T)_m^{+*} \rightarrow (T)_{m-1-x}{\cdot}C_2H_3O^+ + CH_3 + x(T) \qquad (3)$$

$$(T)_m^{+*} \rightarrow (T)_{m-1-x}{\cdot}CH_3^+ + C_2H_3O + x(T) \qquad (4)$$

The loss of neutral fragments proceeds in clusters following ionization in a manner analogous to the processes which occur as a result of the ion–molecule reactions between acetone ion and the neutral acetone monomer.[11,12] In this article, emphasis is placed on the three major cluster ions: $(T)_m{\cdot}H^+$, $(T)_m{\cdot}CH_3^+$, and $(T)_m{\cdot}C_2H_3O^+$ (labeled as Am, Bm, and Cm, respectively, in Figure 2). The unassigned peaks on the left side of the Am and Cm series are the corresponding daughter ion peaks resulting from "bleed-through" in the reflectron of the time-of-flight mass spectrometer.

(a) $(T)_m{\cdot}H^+$. The intensities of protonated acetone cluster ions, $(T)_m{\cdot}H^+$, m = 1–10, are the highest among all of the types of cluster ions with the same number, m, of solvent molecules. Although the experiments were performed under collisionless conditions, the various ion species are subject to dissociation processes. As a consequence, the relative ion intensities of the fragment cluster ions may reflect the relative stability of the clusters. It is interesting to note that Munson has proposed a model[8] which suggested that the disolvated proton species is the most stable ion in the acetone system due to formation of an O–H–O bond. However, MacNeil and Futrell[12] observed that the trisolvated species was also a relatively stable ion; the largest protonated species they reported was the protonated tetramer ion.

In the case of cluster ionization, our results show that the $(T)_m{\cdot}H^+$, m = 1–10, ion intensity decreases smoothly as a function of cluster size (Figure 2). This finding for cluster ionization is in contrast to the earlier results for ion–molecule association reactions. Although drawing a smooth curve through the $(T)_m{\cdot}H^+$ series in the figure may suggest a slightly enhanced intensity for the protonated dimer, the present results do not support any particular cluster ion as being more stable than others in the protonated acetone cluster ion systems.

(b) $(T)_m{\cdot}C_2H_3O^+$. The most abundant fragment species from the ionized acetone monomer is $C_2H_3O^+$; the acetyl cation CH_3CO^+ is the most stable of the various possible isomeric structures.[19,20] The solvated acetyl ions, $(T)_m{\cdot}C_2H_3O^+$, m = 1–17, are present in a significant amount. As seen in Figure 2, their intensities are slightly lower than those of protonated species of the same number of solvent molecules. The $(T)_m{\cdot}CH_3CO^+$ ion intensity is observed to decrease smoothly as cluster size for m = 1–10. As discussed in section 2 below, among different types

(19) Terlouw, J. K.; Heerma, W.; Holmes, J. L. *Org. Mass Spectrom.* **1981**, *16*, 306.

(20) Nobes, R. H.; Bouma, W. J.; Radom, L. *J. Am. Chem. Soc.* **1983**, *105*, 309.

of cluster ions with the same number (three) of solvent molecules, the $(T)_3{\cdot}C_2H_3O^+$ is relatively the most stable.

(c) $(T)_m{\cdot}CH_3^+$. Also seen in Figure 2 is that methylated cluster ions, $(T)_m{\cdot}CH_3^+$, m = 1–10, are formed. However, their intensities are smaller than those of the solvated proton and acetyl species. Nevertheless, their intensity level is sufficient to observe their metastability, a topic which is discussed in section B.

(2) Cluster Ion Size Distributions. Figure 3 displays for the two major cluster ions, as a function of the number of bound solvent molecules, the relative cluster ion intensity normalized to the protonated acetone cluster of the same size. As seen from the figure, the ion intensity ratio $[(T)_m{\cdot}CH_3^+]/[(T)_m{\cdot}H^+]$ is nearly constant at about 0.1. For all but $m \simeq 3$ of the 10-solvent-molecule-containing clusters studied, for m = 1–10 the $[(T)_m{\cdot}C_2H_3O^+]/[(T)_m{\cdot}H^+]$ shows nearly a smooth and slightly increasing ratio, with the values ranging from 0.6 for m = 1 to 0.9 for m = 10. The anomalously high ratio for m = 3 warrants further discussion. First, it should be noted that dividing by $[(T)_m{\cdot}H^+]$ is only for normalization of the data; this procedure does not lead to the appearance of the feature at m = 3, since it would then be apparent in both curves.

There are several factors contributing to the relative cluster ion abundances observed in a conventional TOF mass spectrum: (1) relative concentration of each neutral cluster species of different size, (2) ionization cross sections of neutral cluster species of different size, (3) branching ratios of prompt fragmentation channels of cluster ions, and (4) cluster ion stability. Though the first two factors are not well known, cluster ion size distributions still can give insight into ion fragmentation branching ratios of various channels and relative cluster ion stabilities. Taking into account the experimental uncertainties of ±10%, Figure 3 shows that the ion intensity ratio is independent of cluster size for both $(T)_m{\cdot}CH_3^+$ and $(T)_m{\cdot}H^+$ ions. Our experimental results suggest that the branching ratios for producing these two classes of fragment ions having the same numbers of acetone molecules are comparable. The fact that $[(T)_m{\cdot}C_2H_3O^+]/[(T)_m{\cdot}H^+]$ increases very gradually with increasing cluster size may be due to a slightly enhanced solvation of the core ion $C_2H_3O^+$.

The most pronounced data point in Figure 3 is that of m = 3 in the curve of $[(T)_m{\cdot}C_2H_3O^+]/[(T)_m{\cdot}H^+]$. This observation, then, implies that the $(T)_3{\cdot}C_2H_3O^+$ is a particularly stable ion. Other evidence for the relatively stable $(T)_3{\cdot}C_2H_3O^+$ is the low intensity of its daughter ion, $(T)_2{\cdot}C_2H_3O^+$ as shown in Figure 6. As discussed below, the observation of a low intensity of a daughter ion implies few $(T)_3{\cdot}C_2H_3O^+$ ions undergo unimolecular decomposition, indicating that it is a relatively stable parent ion.

(3) Water Elimination from $(T)_m{\cdot}H^+$. The observed ion peaks at masses 99, 157, 215, 273, and 331, which correspond to $(T)_{m-2}{\cdot}C_6H_{11}O^+$, m = 2–6, are the dehydration products of the protonated species, $(T)_m{\cdot}H^+$, m = 2–6. These $(T)_{m-2}{\cdot}C_6H_{11}O^+$ ions have been seen in the previous studies of ion–molecule reactions[12] in this system. However, Luczynski and Wincel[10] have demonstrated that the protonated acetone can associate with $(CH_3)_2CO$ and H_2O molecules to form the proton-bound species $(T)_m{\cdot}H^+$ through sequential clustering reactions, and $(T)_{m-1}{\cdot}(H_2O){\cdot}H^+$ (with m up to 6) through exchange processes. In addition, the $(T)_m{\cdot}H^+$, $m \geq 2$, decomposes by eliminating a water molecule to form $(T)_{m-2}{\cdot}C_6H_{11}O^+$.

Figure 4a is a portion of the TOF spectrum of the acetone cluster ions in the case where water content in the acetone sample is 0.4% or less. There are not any peaks corresponding to $(T)_3{\cdot}(H_2O)^+$ (mass 192) or $\{(T)_3{\cdot}(H_2O)\}H^+$ (mass 193). One can readily identify the ion peaks at masses 157 and 215 corresponding to the $(T)_{m-2}{\cdot}C_6H_{11}O^+$, $m \geq 2$, ions which clearly originate from the direct elimination of water molecules from the $(T)_m{\cdot}H^+$ via the reaction:

$$(T)_m{\cdot}H^+ \rightarrow (T)_{m-2}{\cdot}C_6H_{11}O^+ + H_2O \qquad (5)$$

Thereafter, experiments were conducted to study the influence of the presence of water in the cluster on the dehydration reactions. Figure 4b shows the same portion of the TOF spectrum of the acetone cluster ions as that in Figure 4a, but, in the case where

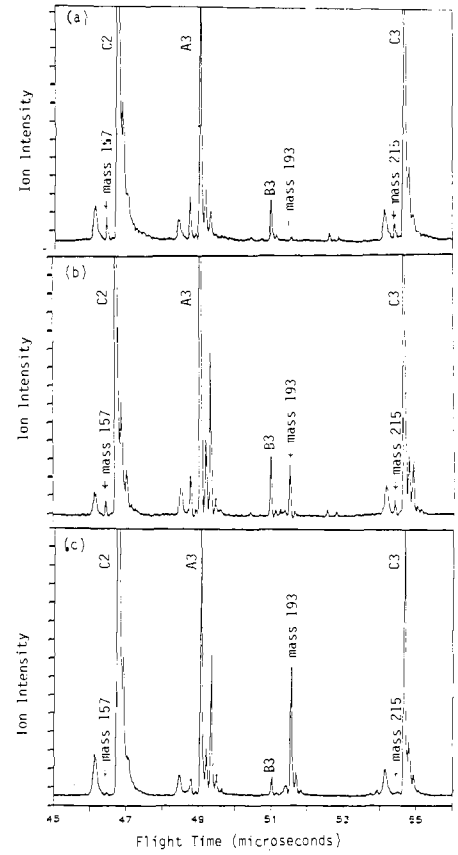

Figure 4. Time-of-flight spectra of acetone cluster ions: (a) 0.4% water in the acetone sample $[(T)_1{\cdot}C_6H_{11}O^+$ (mass 157) and $(T)_2{\cdot}C_6H_{11}O^+$ (mass 215) are seen, whereas ion signal corresponds to $(T)_3{\cdot}(H_2O){\cdot}H^+$ (mass 193) in the mass range shown is not found]; (b) 0.7% water in the acetone sample, (all ion peaks corresponding to masses 157, 215, and 193 are observed); (c) 1.0% water in the acetone sample, [ion peaks corresponding to $(T)_1{\cdot}C_6H_{11}O^+$ (mass 157) and $(T)_2{\cdot}C_6H_{11}O^+$ (mass 215) are not seen; however, $(T)_3{\cdot}(H_2O){\cdot}H^+$ (mass 193) is clearly identified]. $A_{x,y} \equiv Ax \rightarrow Ay$; $B_{x,y} \equiv B_x \rightarrow B_y$; $C_{x,y} \equiv Cx \rightarrow C_y$.

0.7% water is present in the acetone sample, the ion peaks corresponding to the $(T)_{m-2}{\cdot}C_6H_{11}O^+$, m = 3 and 4 (masses 157 and 215), and $\{(T)_3{\cdot}(H_2O)\}H^+$ ion (mass 193) are evident. Furthermore, Figure 4c also displays the same portion of the TOF spectrum of the acetone cluster ions as that in Figure 4a, in the case where water content in the acetone sample is 1.0%. Interestingly, the peak corresponding to the $\{(T)_3{\cdot}(H_2O)\}H^+$ ion (mass 193) is evident, whereas those corresponding to the $(T)_{m-2}{\cdot}C_6H_{11}O^+$ ions are not seen (no peaks appear at either mass 157 or mass 215). The findings strongly suggest that the presence of water inhibits the dehydration mechanism of $(T)_m{\cdot}H^+$ cluster ions.

Reaction 5 has been reported by many researchers[10-12] in the studies of ion–molecule reactions of the gas-phase acetone system. On the contrary, Stace and Shukla[13] did not observe this reaction in studies where the neutral clusters of acetone were ionized by electron impact. They suggested a possible explanation that the structures of the precursor ion $(T)_m{\cdot}H^+$ are different in these two different experiments. However, the results of our present studies have shown that the presence of water molecules in a cluster suppresses the dehydration reaction. Although the authors did not state the extent of water impurity, if any, in their system, our finding provides an alternative explanation for the discrepancy between the two studies mentioned above.

For simplicity, only the dehydration mechanism of the protonated acetone dimer is discussed; see Scheme I. The structure of protonated acetone dimer (I) can be written as a combination of ketone and enol forms, as shown in structure II.[21] The pro-

(21) Sykes, P. *A Guide Book to Mechanism in Organic Chemistry*, 5th ed. Longmans: New York, 1981; p 221.

Scheme I

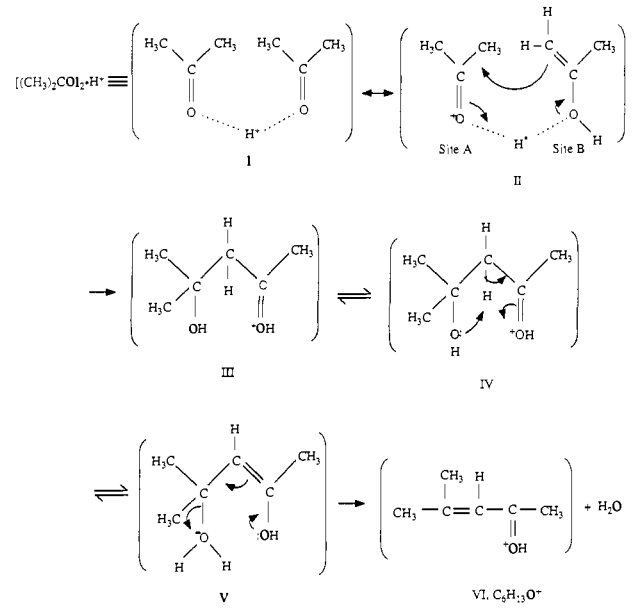

tonated acetone dimer undergoes a common water elimination reaction through intermediate species III–V to yield the protonated mesityl oxide, $C_6H_{11}O^+$ (VI). When water is present in the system, it would bond to site A rather than the OH on site B in structure II. As a result, the dehydration reaction of the protonated acetone cluster is quenched. By contrast, another acetone molecule would only bond to site B.

(B) Studies of Metastable Processes. Studies of metastable decomposition processes occurring in the time-of-flight field-free region are made by collecting corresponding daughter ions while varying potential U_t applied to the middle plate of the reflectron (see Figure 1). Recall that Figure 2 is a TOF spectrum under hard reflection conditions (U_t is higher than the initial parent ion energy U_0). Under such conditions, a conventional TOF spectrum is obtained whereby ions which are accelerated to a terminal velocity arrive at the detector at the same time, irrespective of whether they have subsequently undergone dissociation. Hence, in conventional TOF mass spectrometry, one is not able to distinguish daughter ions from parent ions when there is a metastable decomposition process involved.

Consider a general unimolecular dissociation event represented as follows:

$$P \rightarrow D + N \qquad (6)$$

where P, D, and N represent, respectively, the parent ion, daughter ion, and neutral fragment. The daughter ion energy is then expressed as $U_d = (M_d/M_p)U_0$. One can define the U_c, cutoff potential of the daughter ion, as the lower limit of U_d (since U_o is a distribution). When one lowers the potential U_t on the energy analyzer grid to a value such that U_t is less than U_c, the daughter ions are reflected back from the reflectron unit while parent ions penetrate through the reflectron. This leads to spatial, and therefore temporal separation of parents and daughters, and it is thereby relatively straightforward to identify metastable precursors for each daughter ion peak.

(1) Unimolecular Decomposition of Acetone Cluster Ions. As mentioned previously in the Experimental Section, the initial parent ion energy U_0 has been measured to be 1825 ± 10 V. Figure 5a is a TOF spectrum taken at U_t = 1380 V. Clearly, these ion peaks can be assigned to (1) $(T)_m{\cdot}H^+ \rightarrow (T)_{m-1}{\cdot}H^+$, m = 2–4, designated as $A_{x,y}$ in the figure; (2) $(T)_m{\cdot}CH_3^+ \rightarrow (T)_{m-1}{\cdot}CH_3^+$, m = 2, 3, designated as $B_{x,y}$; (3) $(T)_m{\cdot}C_2H_3O^+ \rightarrow (T)_{m-1}{\cdot}C_2H_3O^+$, m = 1–3, designated as $C_{x,y}$. Another TOF spectrum, taken at U_t = 1360 V, is shown in Figure 5b. One can immediately see the disappearance of the daughter ion peak corresponding to the process; $(T)_4{\cdot}H^+ \rightarrow (T)_3{\cdot}H^+$, $[A_{4,3}]$, whose cutoff potential is 1363 V as compared to that in Figure 5a.

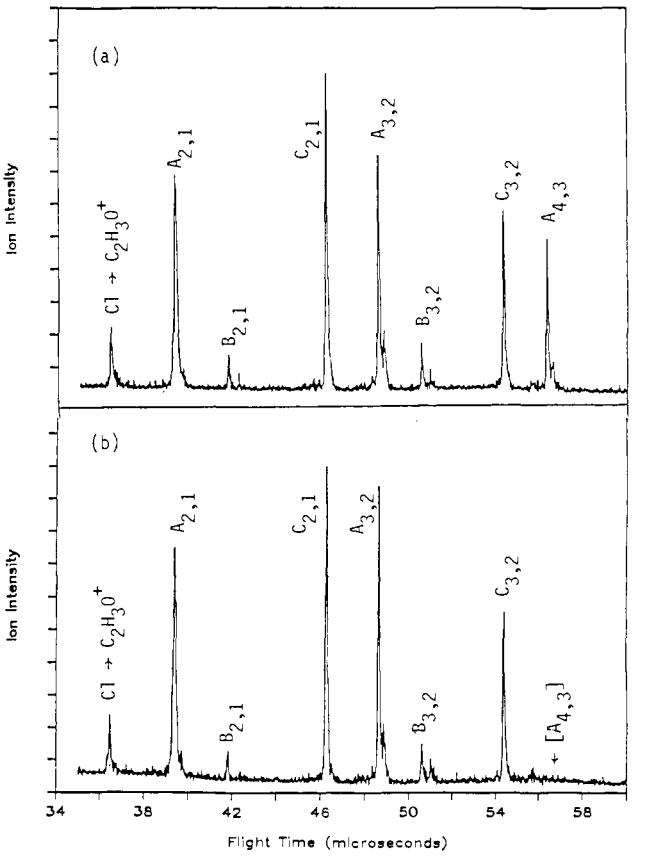

Figure 5. Metastable ion spectra in the acetone cluster ion system. (a) U_t = 1380 V; the metastable peak $A_{4,3}$ of which cutoff voltage is 1363 V is observed. (b) U_t = 1360 V; the metastable peak $A_{4,3}$ disappears since U_t is lower than the cutoff voltage.

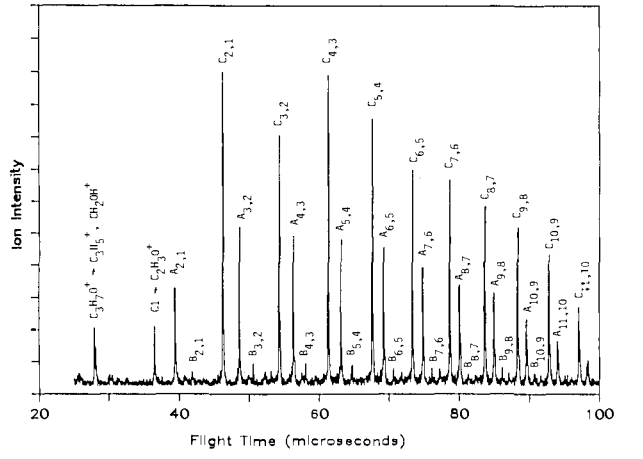

Figure 6. A complete observed metastable ion TOF spectrum, U_t = 1660 V. The unimolecular decomposition processes are described by eq 7–9 in the text.

A complete metastable TOF spectrum, taken at U_t = 1660 V, is shown in Figure 6. A careful scrutinization of the experimental data shows that the metastable decomposition processes for the acetone cluster ions are as follows:

$$(T)_m{\cdot}H^+ \rightarrow (T)_{m-1}{\cdot}H^+ + T \qquad m = 1\text{–}12 \qquad (7)$$

$$(T)_m{\cdot}CH_3^+ \rightarrow (T)_{m-1}{\cdot}CH_3^+ + T \qquad m = 1\text{–}10 \qquad (8)$$

$$(T)_m{\cdot}C_2H_3O^+ \rightarrow (T)_{m-1}{\cdot}C_2H_3O^+ + T \qquad m = 1\text{–}12 \qquad (9)$$

In addition, unimolecular decomposition processes corresponding to $(T){\cdot}H^+ \rightarrow (C_3H_5^+$ and $CH_2OH^+)$ and $C_2H_3O^+ \rightarrow CH_3^+$ (not shown) are also easily identified. There are two different unimolecular decomposition channels observed for the metastable

species $(T)\cdot H^+$. This will be discussed in a separate publication.[22]

Stace[13] has reported process 7 but did not observe process 9 which he attributed to a collision-induced decomposition process. This may indicate that process 9 can occur through both unimolecular decomposition and collision-induced decomposition processes since the present work clearly establishes that process 7 also occurs without collisions.

Summary

Three major types of solvated acetone cluster ions $\{[(CH_3)_2CO]_m\cdot H^+$, $m = 1-15$; $[(CH_3)_2CO]_m\cdot C_2H_3O^+$, $m = 1-17$; and $[(CH_3)_2CO]_m\cdot CH_3^+$, $m = 1-10\}$ are observed following the photoionization of neutral acetone clusters. The results are in agreement with the findings in the gas-phase ion-molecule chemistry and demonstrate further the similarity of the ensuing ion chemistry of cluster ion systems which occur via analogous internal ion-molecule reactions.[17,18,23] In the case of prompt ion fragmentation, the branching ratios for yielding methylated and protonated cluster species are independent of cluster size. However, the normalized intensities of the acetylated to protonated cluster ions (upper curve, Figure 3) show nearly a smooth and slightly increasing trend as a function of cluster size. In the time window of several tens of microseconds, all three major types of cluster ions undergo unimolecular decompositions by "boiling off" one acetone molecule.

The most exciting and striking finding of the present work is that the presence of trace amounts of water in the system inhibits the dehydration mechanism of protonated acetone cluster ions. These findings explain the apparent discrepancy between earlier studies. Most importantly, the results provide further evidence for the influence of solvation on reactions in clusters.[24,25]

Acknowledgment. Financial support by the U. S. Department of Energy, Grant No. DE-FG02-88ER60648, is gratefully acknowledged. The authors also thank Dr. Robert G. Keesee for helpful discussions concerning the work.

Registry No. Acetone, 67-64-1.

(22) Tzeng, W. B.; Wei, S.; Castleman, A. W., Jr. Metastability of Protonated Acetone Cluster Ions, in preparation.
(23) Klots, C. E.; Compton, R. N. *J. Chem. Phys.* **1978**, *69*, 1636.
(24) Morgan, S.; Castleman, A. W.; Jr. *J. Am. Chem. Soc.* **1987**, *109*, 2867.
(25) Garvey, J. f.; Berstein, R. B. *J. Phys. Chem.* **1986**, *90*, 3577.

Temporary Anion States in Nitrosyl Transition-Metal Complexes Studied by Electron Transmission Spectroscopy and Multiple Scattering Xα Calculations

Alberto Modelli,*,† Antonio Foffani,† Francesco Scagnolari,† Sandro Torroni,† Maurizio Guerra,*,‡ and Derek Jones‡

Contribution from the Dipartimento di Chimica "G. Ciamician", Universita' di Bologna, via F. Selmi 2, 40126 Bologna, Italy, and Istituto dei Composti del Carbonio Contenenti Eteroatomi, C.N.R., via della Chimica 8, 40064 Ozzano Emilia (BO), Italy. *Received March 6, 1989*

Abstract: The electron transmission spectra of $Fe(CO)_2(NO)_2$, $Co(CO)_3NO$, and $Ni(\eta^5\text{-}C_5H_5)NO$ have been recorded in the 0-5-eV energy range. The experimental attachment energy values were reproduced by multiple scattering (MS) Xα calculations, using the transition-state procedure. The calculations also predicted four stable anion states in the iron complex and two stable anion states in the cobalt complex. The experimentally observed stabilization of the anion states with prevailing ligand character, with respect to the corresponding anion states in the free ligands, has been found to be consistent with the calculated charge densities in the neutral states, according to which the central metal has a large negative charge, owing to the acceptor capability of the empty 4s and 4p orbitals. The total electron-scattering cross sections have been calculated with the continuum MS-Xα method.

A knowledge of ionization energies (IEs), electron affinities (EAs), and spatial distributions of frontier molecular orbitals (MOs) is relevant for a better understanding of the chemical bond. The valence occupied MOs of transition-metal complexes have been extensively characterized in energy and nature by UV photoelectron spectroscopy and theoretical studies. The complementary information on the vacant energy levels, however, is scarce.

Electron transmission spectroscopy (ETS)[1] is one of the most powerful means for measuring the various vertical EAs of gas-phase molecular systems. This electron-scattering technique takes advantage of the sharp variations in the total electron-scattering cross section caused by resonance processes, that is, formation of temporary anion states. The energies (AEs) at which electron attachment occurs are the negative of the EAs, and, in a Koopmans' theorem sense, they can be associated with the energies of the empty MOs.

We have recently applied ETS to bis π-ligand,[2,3] mixed π-ligand and carbonyl,[4] and carbonyl[5] complexes. The assignment of the resonances observed in the ET spectra to the corresponding anion states was supported by MS-Xα calculations, using the transition-state procedure, which accurately reproduced the experimental EA and IE data, and described the localization properties of the ion states. The significant stabilization of the anion states with

† Universita' di Bologna.
‡ Istituto dei Composti del Carbonio Contenenti Eteroatomi.

(1) Schulz, G. J. *Rev. Mod. Phys.* **1973**, *45*, 378.
(2) Modelli, A.; Foffani, A.; Guerra, M.; Jones, D.; Distefano, G. *Chem. Phys. Lett.* **1983**, *99*, 58.
(3) Burrow, P. D.; Modelli, A.; Guerra, M.; Jordan, K. D. *Chem. Phys. Lett.* **1985**, *118*, 328.
(4) Modelli, A.; Distefano, G.; Guerra, M.; Jones, D. *J. Am. Chem. Soc.* **1987**, *109*, 4440.
(5) Guerra, M.; Jones, D.; Distefano, G.; Foffani, A.; Modelli, A. *J. Am. Chem. Soc.* **1988**, *110*, 375.

0002-7863/89/1511-6040$01.50/0